ADVANCED FUNCTIONAL MATERIALS
www.afm-journal.de

Porous Silicon-Based Optical Microsensors for Volatile Organic Analytes: Effect of Surface Chemistry on Stability and Specificity

By *Anne M. Ruminski, Brian H. King, Jarno Salonen, Jay L. Snyder,* and *Michael J. Sailor**

Sensing of the volatile organic compounds (VOCs) isopropyl alcohol (IPA) and heptane in air using sub-millimeter porous silicon-based sensor elements is demonstrated in the concentration range 50–800 ppm. The sensor elements are prepared as one-dimensional photonic crystals (rugate filters) by programmed electrochemical etch of p^{++} silicon, and analyte sensing is achieved by measurement of the wavelength shift of the photonic resonance. The sensors are studied as a function of surface chemistry: ozone oxidation, thermal oxidation, hydrosilylation (1-dodecene), electrochemical methylation, reaction with dicholorodimethylsilane and thermal carbonization with acetylene. The thermally oxidized and the dichlorodimethylsilane-modified materials show the greatest stability under atmospheric conditions. Optical microsensors are prepared by attachment of the porous Si layer to the distal end of optical fibers. The acetylated porous Si microsensor displays a greater response to heptane than to IPA, whereas the other chemical modifications display a greater response to IPA than to heptane. The thermal oxide sensor displays a strong response to water vapor, while the acetylated material shows a relatively weak response. The results suggest that a combination of optical fiber sensors with different surface chemistries can be used to classify VOC analytes. Application of the miniature sensors to the detection of VOC breakthrough in a full-scale activated carbon respirator cartridge simulator is demonstrated.

1. Introduction

The use of porous Si has been explored for various environmental sensing applications. The photoluminescence,[1–3] refractive index[4,5] and dielectric constant[6,7] of porous Si are very sensitive to the presence of molecules in the pores. Volatile organic compounds,[1,5,8] explosives[9] and polycyclic aromatic hydrocarbons[10] have all been detected, with detection limits of a few ppb reported for some of these compounds.[11]

Porous Si offers many advantages as a chemical sensing platform. The porous layer contains a high specific surface area for analyte adsorption (in the range of a few hundred m^2 per cm^3).[12] The surface chemistry can be tailored,[13] and the porous layer is easy to produce.

Porous Si photonic crystals can be fabricated from highly doped p-type silicon by applying a sinusoidal anodic current during an electrochemical etch. This etching waveform produces a porous film with a periodic modulation in porosity and refractive index in the <100> direction of the silicon wafer, resulting in an optical structure known as a rugate reflector.[14] The reflectivity spectrum contains a sharp spectral peak at a wavelength corresponding to the period of the sinusoidal etching waveform. Reflectivity peak wavelengths are also dependent on the refractive index of the porous film. When a substance enters the pores the refractive index of the porous layer increases, producing a red shift in the reflectivity peak. The shift of the reflectivity peak provides a means to quantify the amount of chemical in an analyte matrix.

The chemical functionality of the surface species dictates the response and the stability of the porous Si sensor.[13,15,16] In particular, grafting of chemical functionalities via formation of Si-C bonds has been found to be a convenient means to prepare stable sensors that display a degree of chemical selectivity. Grafting can be achieved by electrochemical reduction of alkyl halides[17] or by hydrosilylation of terminal alkenes.[18–20] Whereas the native surface of porous Si contains hydrophobic, air-reactive Si-H species, grafting of aliphatic hydrocarbons generates a similarly hydrophobic but significantly more stable surface. Using aliphatic compounds that contain specific functional groups such as carboxylate provides a means to incorporate different surface affinity properties while retaining the chemical stability of the Si-C bonded sensor surface.[21] A carbonaceous species can also be grafted to the porous Si surface by thermal decomposition of acetylene on a native porous Si

[*] A. M. Ruminski, B. H. King, Prof. M. J. Sailor
Department of Chemistry and Biochemistry
The University of California
San Diego, 9500 Gilman Drive
La Jolla, CA 92093–0358 (USA)
E-mail: msailor@ucsd.edu
J. Salonen,
Department of Physics
University of Turku
FI-20014, Turku (Finland)
Jay L. Snyder,
National Institute of Occupational Safety and Health
NIOSH/NPPTL, Pittsburgh, PA 15236 (USA)

DOI: 10.1002/adfm.201000575

surface.[22] Although less well-defined than the hydrosilylation route, the "hydrocarbonized" porous film is environmentally stable[23] and its chemical sensing capabilities have been demonstrated.[24–27]

In this work, we prepare porous Si rugate reflectors with the different chemical modifications described above, and quantify the optical reflectivity response of the photonic crystals to hydrophilic (isopropanol) and hydrophobic (heptane) analytes. The stability of each sensor type is quantified for a period of 15 days. From this screen, two sensor chemistries (thermal oxide and acetylene carbonization) with acceptable stability and displaying significantly different analyte responses are incorporated into porous Si microparticles that are then attached to the tips of optical fibers. The suitability of the fiber-based microsensors in a remote sensing application is demonstrated. We find that microsensors modified with acetylene effectively minimize interference from fluctuations in relative humidity.

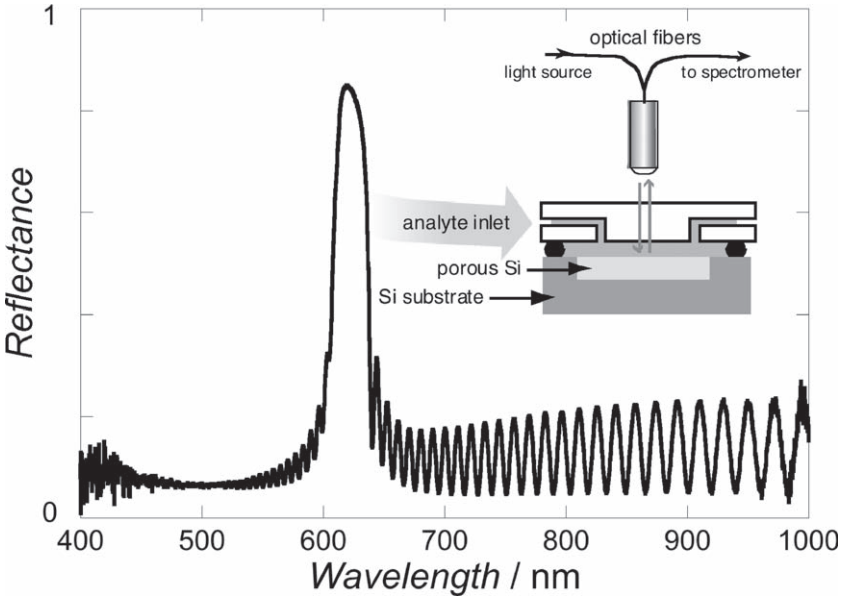

Figure 1. Typical reflectance spectrum of the porous Si rugate filters used in this study, and a diagram of the experimental setup used for vapor sensing. The sample is etched using a sine wave, which results in a one-dimensional photonic crystal. This spectrum is of a native surface (Si-H terminated) sample. The reflectance spectrum is acquired at normal incidence, as indicated in the inset.

2. Results and Discussion

2.1. Preparation and Characterization of Porous Si Photonic Crystals

Porous Si samples were prepared by electrochemical etch of highly doped p-type silicon in an ethanolic HF solution. The current was varied sinusoidally, producing a film containing layers with gradually modulated porosity.[14,28] The layered structure acts as a one-dimensional photonic crystal known as a rugate filter, displaying a peak in the reflectance spectrum whose wavelength is determined by the period of the sine wave used in the etch. All samples were etched with the same minimum and maximum current density, HF concentration and etch duration, and the current periodicity was adjusted in order to produce a reflectance peak located at ~650 nm after chemical modification (**Figure 1**).

Sample porosity was determined by gravimetric analysis.[29] Samples were weighed before etching, after etching and after dissolution of the porous layer with a 0.1 M KOH solution in water and ethanol. Four sample etch types were prepared for porosity analysis: a rugate reflector etched with a period of 10 s, a rugate reflector etched with a period of 11.5 s, a single stack etched at the lowest current density value used for the rugate reflectors, and a single stack etched at the highest current density value used for the rugate reflectors. Porous layer thickness was measured by cross-sectional scanning electron microscopy (SEM). The average porosity and thickness of each sample is given in **Table 1**.

The various chemical modification reactions were performed immediately after etching the samples. Nine different chemical reactions from the literature were employed to generate distinct surface functionalities. **Table 2** summarizes the chemical reaction chemistries, the idealized type of surface it generates, and the measured sessile drop contact angles. Representative attenuated total reflectance Fourier transform infrared (ATR-FTIR) spectra are given in Supplemental Figure 1. The oxidation methods all tend to generate hydrophilic surfaces. Ozone oxidation produces a more hydrophilic surface than thermal oxidation, presumably due to the presence of a larger amount of surface Si-OH species. The ATR-FTIR spectra support this interpretation; along with the asymmetric Si-O-Si and Si-O stretching vibrations at 1025 cm^{-1} and 780 cm^{-1}, respectively, a strong band assigned to ν O-H is observed at 3350 cm^{-1} for the ozone-oxidized material. This species is detected as a minor component in the ATR-FTIR spectrum of the thermally treated material. At the temperature used in the thermal oxidation reaction, hydroxylated (Si-OH)

Table 1 Porosity and Thickness of Porous Si Samples[a]

Sample	Porosity (%)[b]	Thickness (μm)[c]
Rugate, 10s period	74.2 ± 0.6	13.27 ± 0.06
Rugate, 11.5s period	75.6 ± 0.7	13.5 ± 0.1
Single layer, 13.3 mA/cm^2	66 ± 2	–
Single layer, 66.4 mA/cm^2	76.9 ± 0.6	–

[a] All samples prepared using a 3:1 v:v solution of aqueous hydrofluoric acid:ethanol. Rugate layers were etched using a sinusoidal current density waveform varying between 13.3 and 66.4 mA/cm^2. All layers were etched for a duration of ~10 min. [b] Gravimetric measurement. Errors represent 1 standard deviation from 5 measurements. [c] Cross-sectional SEM measurement of cleaved samples. Errors represent 1 standard deviation from 3 measurements.

Table 2 Surface Chemistries Prepared on Porous Si Samples[a]

Process	Chemical Reaction	Surface Species	Contact Angle (°)[b]	r = Δλ(Heptane)/ Δλ(Isopropanol)
Native surface	–	Si-H	102 ± 3	0.74
Ozone oxidation*[53]*	Si-H + O_3 =>	Si-O-Si, Si-OH	11 ± 1	0.053
Thermal oxidation (600 °C, 90 m)*[54]*	Si-H + O2 =>	Si-O-Si	20 ± 1	0.11
Hydrosilylation with 1-dodecene*[34]*	Si-H + CH_2=$CH_2(CH_2)_9CH_3$ =>	Si-$(CH_2)_{11}CH_3$	119 ± 2	0.69
Electrochemical methylation*[17]*	Si-H + CH_3I =>	Si-CH_3	102 ± 3	0.92
Ozone oxidation + dichlorodimethylsilane*[16]*	(a) Si-H + O_3 => Si-OH	Si-O-Si$(CH_3)_2$-O-Si	101 ± 1	0.49
	(b) 2 Si-OH + $Cl_2Si(CH_3)_2$ =>			
Thermal acetylation (300 °C, 30 m)*[23]*	Si-H + H-C≡C-H =>	"Si-C"	53 ± 3	0.75
Thermal acetylation (485 °C, 30 m)*[23]*	Si-H + H-C≡C-H =>	"Si-C"	80 ± 3	5.0
Thermal acetylation (500 °C, 30 m)*[23]*	Si-H + H-C≡C-H =>	"Si-C"	76 ± 7	2.9

[a] Attenuated total reflectance Fourier transform infrared (ATR-FTIR) spectra of all samples are included in Supplemental Figure 1. Surface species shown in the table are meant to represent idealized surface chemistry. Many of the reactions also generate oxide concomitant with the modification reaction. [b] Contact angle measurements were performed on the same day as chemical functionalization.

surfaces are known to undergo dehydration to generate the more hydrophobic Si-O-Si surface.[30–32] The asymmetric Si-O-Si and Si-O stretching vibrations for the thermally oxidized material appear in the FTIR spectrum at 1033 and 808 cm^{-1}, respectively.

Several of the chemical modification methods of Table 2 result in hydrophobic material, by placing either aliphatic hydrocarbons or silicon carbide-like species on the surface. The silicon carbide-like species are generated by pyrolysis of acetylene on the surface of a freshly prepared (hydrogen-terminated) porous Si chip. Previous studies report that the temperature of the pyrolysis reaction plays a key role in determining the degree of hydrophobicity or hydrophilicity of the resulting "hydrocarbonized" porous film.[27,33] In this study, three different pyrolysis temperatures (300, 485 and 500 °C) were used to prepare hydrocarbonized samples. For all of the preparations, ATR-FTIR spectra display a prominent broad band at 1000 cm^{-1}. This band appears in a region of the FTIR spectrum (1050–1150 cm^{-1}) that is generally associated with silicon oxides. However, the band remained after samples were soaked in an ethanolic solution of HF, suggesting that the band cannot be due to oxide (silicon oxides rapidly dissolve in HF solutions). On the basis of density functional theory calculations, Salonen and coworkers assigned the 1000 cm^{-1} band of thermally carbonized porous Si to C-H vibrations from a species in which the carbon atom is back-bonded to Si atoms.[23] This assignment is consistent with the other bands observed in the FTIR spectrum, which include C-H stretching (~2900 cm^{-1}) and bending (~1385 cm^{-1}) vibrations.[22]

Contact angle measurements of the actetylene-treated, hydrocarbonized samples were less consistent than with the other chemical modifications. The water contact angle was observed to decrease as a function of time, and the footprint of the drop on the sample was often not round. We ascribe this to surface heterogeneity; presumably the acetylation chemistry produces a mixture of hydrophobic and hydrophilic domains.

Three chemical modification methods were used to place aliphatic hydrocarbon species on the porous Si surface: a long hydrocarbon chain was bonded to the surface through a thermal hydrosilylation reaction with 1-dodecene,[34] a methyl group was attached by electrochemical reduction of methyl iodide, and a dimethylsiloxy group was attached by thermal reaction of an ozone-oxidized sample with dichlorodimethylsilane. ATR-FTIR spectra confirmed the presence of the aliphatic or methyl species. The aliphatic species displayed bands assigned to C-H stretching and deformation modes at 2966, 2926, 2858 and 1469 cm^{-1}, and the methyl-capped surfaces displayed a distinctive band associated with the methyl rocking mode at 769 cm^{-1}.[17] Both of the surface preparations that produce surface-bound methyl species (electrochemical reduction of CH_3I or reaction with dichlorodimethylsilane) generate material that displays the same contact angle.

2.2. Effect of Chemical Modification on Analyte Response

The relative hydrophobicity of chemically modified porous Si chips was evaluated by comparing the optical response of each sample to isopropanol and to heptane vapors. Each of the two analytes was introduced individually into a nitrogen stream at a concentration of 500 ppm. The reflectivity peak maximum of the 1-D photonic crystal of porous Si was determined using a Gaussian fit, and the wavelength shift of the reflectivity peak was recorded (**Figure 2**). The response of a given sample to heptane is divided by the response to isopropanol, producing a response factor "r" as defined in Equation 1.

$$r = \frac{\Delta\lambda_{\text{heptane}}}{\Delta\lambda_{\text{isopropanol}}} \quad (1)$$

Calculated r values of the chemically modified porous Si chips are listed in Table 2. Larger values of r indicate a greater degree of hydrophobicity. As might be expected from the relatively large quantity of surface Si-OH species, ozone-oxidized samples display the smallest r value (0.053), followed closely by thermally oxidized samples (0.11). This result is in agreement

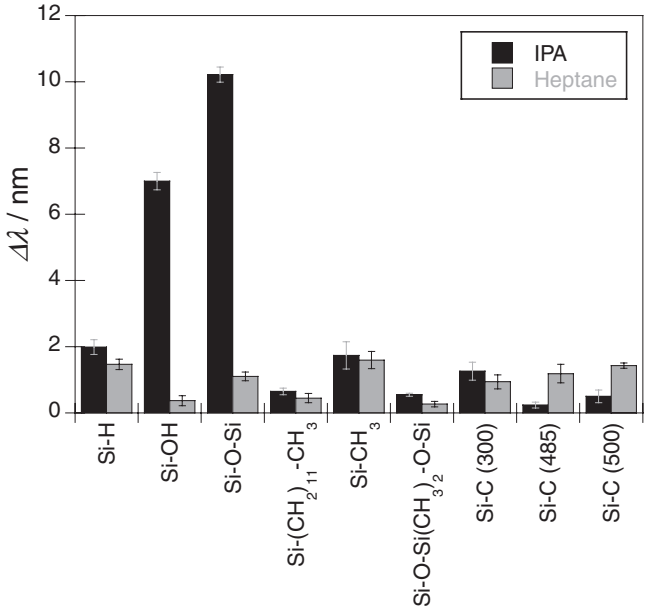

Figure 2. Response of chemically modified porous Si photonic crystal samples to isopropanol (IPA) and heptane vapors. Vertical bars indicate the increase in wavelength ($\Delta\lambda$) of the resonant spectral peak of the photonic crystal relative to the sample in pure N_2, for the indicated surface chemistries. Simplified surface chemistries are described in Table 2: Si-H (native surface of porous Si); Si-OH (ozone oxidized); Si-O-Si (thermally oxidized at 600 °C); Si-$(CH_2)_{11}CH_3$ (hydrosilylated with dodecene); Si-CH_3 (electrochemically methylated); Si-O-Si$(CH_3)_2$-O-Si (modified with dimethylsiloxane); Si-C (acetylated at the indicated temperature, in °C). Analyte concentrations are 500 ppm isopropanol and 500 ppm heptane. Values are the average of 5 samples; error bars represent one standard deviation.

with water contact angles, where ozone-oxidized samples had the smallest contact angle followed by thermally oxidized.

Other samples with r values less than 1.0 include chips that were: acetylated at 150 °C or at 300 °C; reacted with dichlorodimethylsilane; functionalized with dodecene; electrochemically methylated; or unmodified (presenting a native, hydride-terminated porous Si-H surface). Water contact angle measurements on hydride-terminated porous Si indicate a relatively hydrophobic surface, however the value of contact angle steadily decreases upon exposure to air, indicative of slow oxidation of the surface hydrides to produce hydrophilic Si-O-Si and Si-OH species. Samples that were electrochemically methylated and surfaces modified with 1-dodecene displayed the same or a larger water contact angle, respectively, relative to the native Si-H samples. ATR-FTIR spectra of these samples reveal the presence of residual Si-H species on these surfaces. As with the as-etched porous Si-H samples, air oxidation is expected to generate surfaces that are less hydrophobic than expected.

Although the samples reacted with dichlorodimethylsilane and the electrochemically methylated samples displayed the same water contact angle, the dimethylsiloxy terminated samples exhibit a significantly smaller r value than the methyl terminated samples. We attribute this difference to the presence of the Si-O bonds attaching the dimethylsilyl species to the surface and the underlying oxidized porous Si material. Liquid water only probes the hydrophobic methyl groups on the outermost layer, whereas water vapors can penetrate to the more hydrophilic oxides. The electrochemically methylated material has much less oxide and so is expected to exhibit hydrophobic characteristics to both liquid and gas phase water. The water contact angles of the thermally acetylated samples showed no obvious correlation with the measured r value, attributed to the surface heterogeneity produced by the acetylation reaction.

Only two samples exhibited r values greater than 1.0: the acetylated samples prepared at 500 °C (r = 2.9) and at 485 °C (r = 5.0). The ATR-FTIR spectra of the samples prepared at 485 °C displayed more intense C-H stretches at 3055 and 2900 cm^{-1} than samples prepared at 500 °C, indicative of a greater degree of hydrophobicity that is consistent with the relative r values measured and previous studies.[35] Acetylated samples prepared at temperatures >500 °C appear black and lack a discernable photonic peak in the reflectivity spectrum. Salonen and coworkers have proposed that the reaction of acetylene with porous Si at temperatures >500 °C could lead to significant carbonization,[23] and the black appearance is attributed to carbonaceous deposits on the porous Si surface.

2.3. Stability of Chemically Modified Porous Si Sensors

The reproducibility of the vapor response of the chemically modified porous Si wafers was examined over a period of 15 days. Seven of the ten surface types were studied: native surface (Si-H), ozone oxidized (Si-OH), thermally oxidized (Si-O-Si), dodecyl terminated (Si-$(CH_2)_{11}CH_3$), methyl terminated (Si-CH_3), dimethylsiloxy terminated (Si-O-Si$(CH_3)_2$-O-Si), and acetylated at 485 °C (Si-C). Samples were stored in the open laboratory atmosphere and then exposed to 500 ppm of isopropanol and heptane vapors 1, 8 and 15 days after chemical modification. **Figure 3** displays the average responses and r value of each chemically modified sample. ATR-FTIR spectra were acquired for every sample on each of the three sampling days.

Samples with the native Si-H surface displayed no significant change in their response to isopropanol or heptane over the 15-day period, although ATR-FTIR spectra of the native samples displayed an increase in the band associated with Si-O-Si stretching vibrations at 1050 cm^{-1}. Ozone oxidized samples displayed no change in analyte response or in the ATR-FTIR spectrum, within the error limits of the experiments. Thermally oxidized samples displayed an increase in response to isopropanol during the first 8 days, though the response was stable from that point on. No significant change was observed in the heptane response. No detectable changes were apparent in the ATR-FTIR spectra during the 15-day period.

Samples modified with dodecyl, methyl and dimethylsiloxy groups retained the same response to heptane and isopropanol vapors within the error limits for the duration of the 15-day test. However, ATR-FTIR spectra of dodecyl modified samples displayed prominent Si-O-Si and C-H bands at day 1, which decreased in intensity by day 8. No further changes in the ATR-FTIR spectra were noted at day 15. ATR-FTIR spectra of electrochemically methylated samples showed a slight growth of the oxide band at 1050 cm^{-1}, while spectra of the dimethylsiloxy modified samples remained the same over the 15-day period.

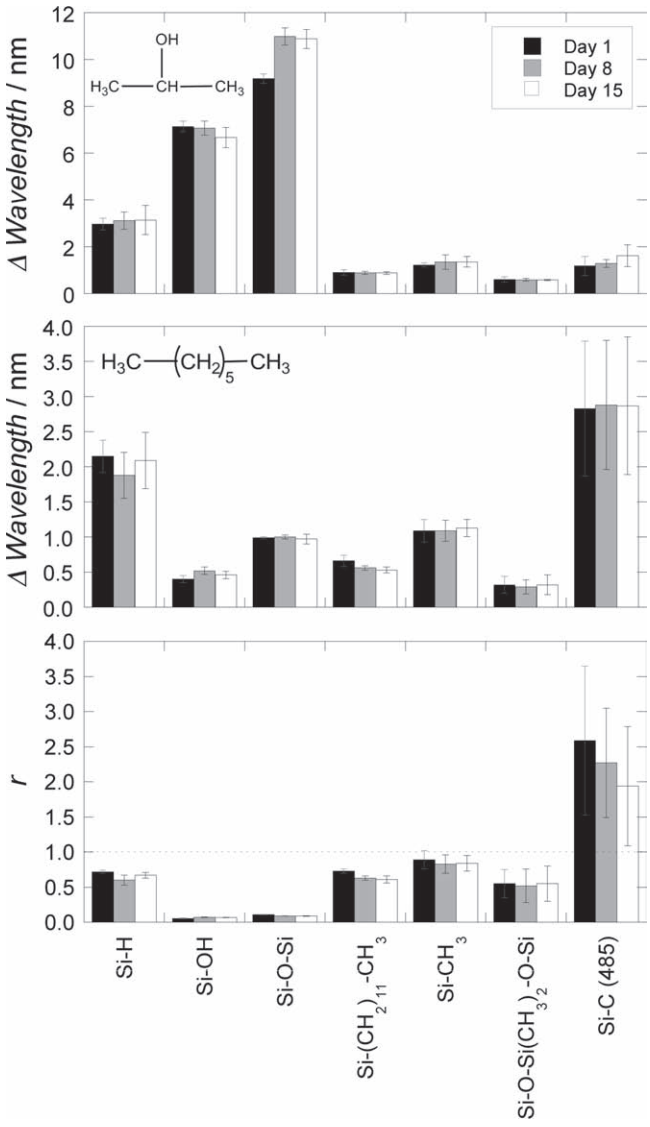

Figure 3. Response of chemically modified porous Si photonic crystal samples to isopropanol and heptane vapors as a function of storage time (in air). Top and Middle: Vertical bars indicate the increase in wavelength ($\Delta\lambda$) of the resonant spectral peak of the photonic crystal upon exposure to 500 ppm isopropanol (Top) or 500 ppm heptane (Middle), for the indicated surface chemistries. Responses measured on day 1 (black bar), day 8 (grey bar) and day 15 (white bar). Bottom: r value (see Equation 1). Horizontal dashed line at r = 1.0 separates samples that display a greater response to heptane (r > 1) from those that display a greater response to isopropanol (r < 1). Values are the average of 5–6 samples; error bars represent one standard deviation. Simplified surface chemistries are described in Table 2: Si-H (native surface of porous Si); Si-OH (ozone oxidized); Si-O-Si (thermally oxidized at 600 °C); Si-$(CH_2)_{11}CH_3$ (hydrosilylated with dodecene); Si-CH_3 (electrochemically methylated); Si-O-Si$(CH_3)_2$-O-Si (modified with dimethylsiloxane); Si-C (485) (acetylated at 485 °C).

Overall the average heptane and isopropanol response of samples reacted with acetylene at 485 °C remained the same within the error limits throughout the 15-day study. However there was a large variation in analyte response between individual samples, leading to the large error bars in the data shown in Figure 3. We attribute this variation to surface heterogeneity, which was also evident in the water contact angle measurements. Surface heterogeneity could possibly be minimized with appropriate optimization of the acetylation procedure. For example, Jalkanen and coworkers place samples in a sealed quartz tube under a flow of nitrogen followed by acetylene prior to placement of the sample and tube into a furnace.[36]

2.4. Remote Sensors by Attachment of Free-Standing Porous Si Films to Optical Fibers

The interior of a carbon filter cartridge is one example of a volume-constrained sensing environment;[37] there are many other instances in which a small sensor form factor is required. The chip-based porous Si sensors discussed so far have a diameter of ~1.2 cm. Previous work has shown that the active porous sensing layer can be removed from the Si substrate and fractured into particles of ~50 μm diameter.[38,39] Referred to as "smart dust," the small particles retain the gas adsorption properties and sensing capability of the original chip-mounted films.[28] In this work, such free-standing porous Si particles were attached to the tip of 600 micron diameter optical fibers (**Figure 4**) as previously demonstrated.[37] The process produces no significant change in the reflectivity spectrum relative to the original chip-based sensors. The small size of the optical fibers allows multiple sensor probes to be placed in a remote location of limited space.

To better differentiate between classes of environmental toxins, three porous Si surface chemistries covering a range of hydrophobic/hydrophilic characteristics were chosen. Chemical modifications that displayed large differences in their relative analyte responses, based on r values, were used in the fiber-based sensor experiments: native surface porous Si (Si-H, r = 0.74), thermally oxidized (Si-O-Si, r = 0.11), and thermal acetylation at 485 °C (Si-C, r = 5.0). Because the acetylation chemistry was highly variable, a single batch of acetylated porous Si films were used for all the fibers in this study.

Porous Si photonic crystals were etched as described in section 2.1. After etching, the porous layer was removed from the bulk Si using an electropolishing etch. The free-standing porous Si films were then immediately functionalized by a thermal treatment in either air (Si-O-Si) or acetylene (Si-C) as described in section 2.2, or they were left unmodified (Si-H). Optical fiber was cleaved to a desired length, stripped partially of the outer cladding layer, and polished on aluminum oxide lapping film to provide a smooth tip for optimal light coupling. The free-standing 50 μm diameter porous Si particles were attached to the tips of the fibers using a partially cured bisphenol A epoxy/modified aliphatic amine curing agent mixture and allowed to cure at room temperature for two days before use.

2.5. Calibration of Porous Silicon-Tipped Fibers with Isopropanol, Heptane, and Relative Humidity

The distal end of each porous Si-tipped optical fiber was fed into a splitter, where one arm went to a light source and the other

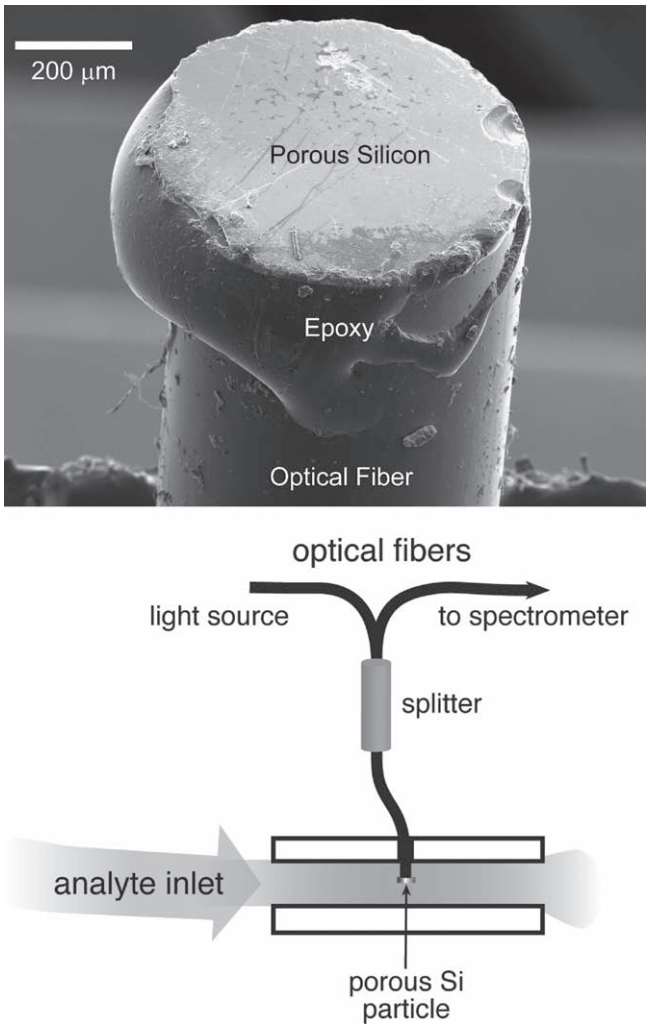

Figure 4. (Top) Scanning electron microscope (SEM) image of an optical fiber capped with a porous Si vapor sensor (rugate filter). The porous Si layer was prepared as a free-standing film and attached to the glass fiber with epoxy. (Bottom) Schematic depicting the optical configuration used for remote sensing.

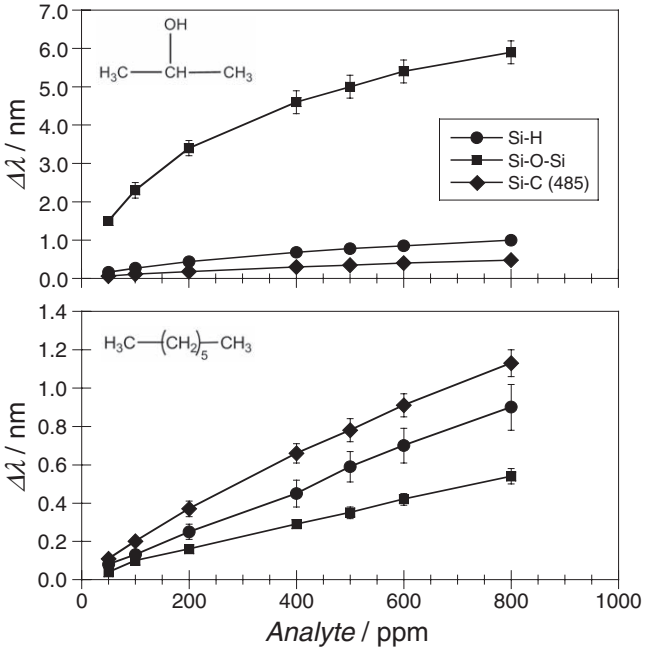

Figure 5. Dose-response curves for fiber-mounted optical porous Si sensors exposed to the analytes isopropanol (top plot) and heptane (bottom plot). Surface chemistries on the porous Si samples were: hydrogen-terminated (Si-H, circles), thermally oxidized (Si-O-Si, squares) or thermally reacted with acetylene at 485 °C (Si-C, diamonds). Lines between points are included as a guide to the eye. Values displayed represent an average of 6–9 samples, error bars correspond to 1 standard deviation.

to a CCD spectrometer. Thus the spectrum of light reflected from the porous Si sensor could be monitored from the backside of the particle, leaving the other end open to access the analyte vapors (Figure 4B). The sensors were calibrated with isopropanol and heptane vapors in an air ambient. Reflectivity peak maxima were recorded in air at ~36% relative humidity and room temperature. Then, analyte concentrations of 50, 100, 200, 400, 500, 600 and 800 ppm were introduced sequentially, with an air purge in between each dose to return the sensor response to the initial baseline reading. Results are displayed in **Figure 5**. As expected, exposure to isopropanol produces the largest wavelength shift in the Si-O-Si sample, followed by Si-H and lastly Si-C. The wavelength shift measured for the Si-H and Si-C samples is linear with analyte concentration. The Si-O-Si sample response curve increases sharply at lower concentrations, but the slope decreases at higher concentrations. All three surface chemistry types display a relatively linear response to heptane vapor. Si-C samples display the greatest change in reflectivity peak wavelength upon exposure to heptane, followed by Si-H and then Si-O-Si. The magnitude of the analyte response of the fiber-mounted porous Si particles (Figure 5) is somewhat less than the response of the chip-based materials (Figure 3) for all the analytes and chemical modifications we tested. This decreased response is attributed to partial infiltration of components of the epoxy used to attach the particles to the optical fibers.

The permissible exposure limits (PEL) for volatile organic compounds published by the Occupational Safety and Health Administration (OSHA) is generally reported as a time weighted average (TWA), where the value is the average VOC exposure limit over a set time (usually eight hours). The OSHA PEL (TWA) for isopropanol is 500 parts per million (ppm),[40] and for heptane it is 500 ppm.[40] As shown in Figure 5, the fiber-mounted porous Si sensors are capable of detecting these analytes at lower concentrations than the two OSHA PELs.

To probe the effects of relative humidity (RH) on the porous Si capped fiber sensors, samples were exposed to stepped increments of ~5% RH beginning at a RH ~41.5% (**Figure 6**) in air. Due to the long time required to remove residual humidity from the dosing system components, purging of the samples was not performed in between different RH increments. Thus the hysteresis of sample response was not examined. The response curves are similar to the isopropanol curves: the oxidized Si-O-Si sample displays the largest response. Si-H samples display the next largest response, followed by Si-C

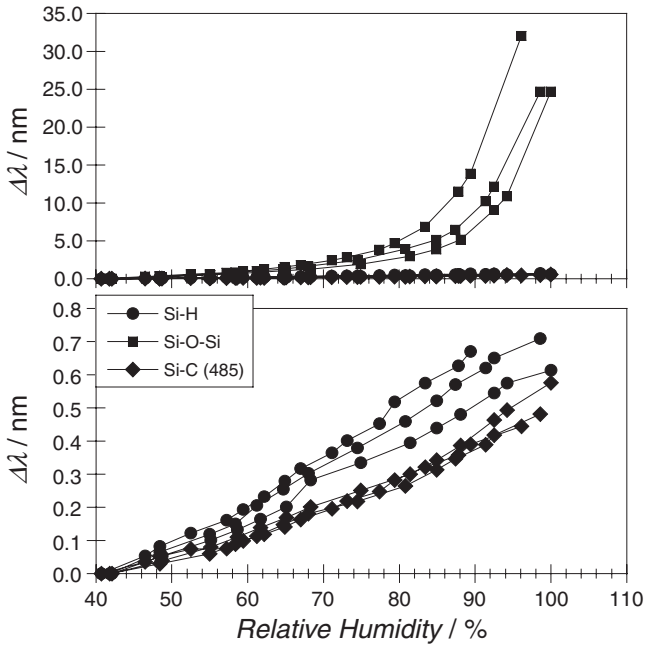

Figure 6. Response of fiber-mounted optical porous Si sensors to relative humidity (RH). Samples are: native surface porous Si (Si-H, gray circles), thermally oxidized (Si-O-Si, black squares) and thermally reacted with acetylene at 485 °C (Si-C, black diamonds). All data points represent the change in wavelength of the reflectivity peak as a function of RH, relative to the wavelength value at RH = 41.5%. Data from 9 samples are shown, representing 3 samples for each of the 3 different surface chemistries. (Top) Chart comparing all three sample types. (Bottom) Plot expanded along the y-axis, showing only the Si-H and the Si-C samples.

samples. The dose-response curves of Si-H and Si-C samples are approximately linear; Si-O-Si exhibits a decrease in sensitivity with increasing concentration. Figure 6 (top) compares the response of the 3 surface chemistries. Relative humidity exerts a large effect on the reflectivity peak position of the oxidized sample, producing a total wavelength shift of 30 nm when relative humidity changes from 41.5% to 99%. By comparison, the more hydrophobic Si-H and Si-C samples display relatively minor responses of <0.8 nm over the same relative humidity change. The results are consistent with the measured sessile drop water contact angle measurements, where thermally oxidized (Si-O-Si) chips show a small contact angle of 20°, while the corresponding value for Si-H is 102°.

2.6. Remote Sensing Application: Detection of Analyte Breakthrough in Activated Carbon Respiratory Cartridges

Optical fibers with chemically responsive sensor heads on their distal end are widely used as remote sensors[41–44] for detecting vapor-phase organic compounds,[42,45] relative humidity[45] and aqueous biomolecules.[46–48] The small form factor (diameters of a few hundred microns and active regions < 1 mm) allows their use in volume-constrained applications, such as the activated carbon filtration cartridge of an air purifying respirator (APR).[37,49] Health and safety regulations in the United States require the use of end-of-service life (ESL) indicators on APRs but allow for the use of service life calculators.[50,51] However, these calculators may require a level of expertise not present in many industrial settings and are subject to the variability of environmental conditions which could result in overexposure to vapor contaminants. End-of-service life indicator cartridges would improve the safety of the APR user by shifting the burden of service life determination from the user to an electronic ESL system.[50,51]

Previously we demonstrated that native porous Si (Si-H)-capped optical fibers can be used to detect analyte breakthrough in a small ampoule packed with activated carbon.[37] Although it demonstrated proof-of-principle, the Si-H chemistry used in that work is not sufficiently stable to be of practical use. In the present work, we find that chemically modified porous Si-capped fibers display improved stability under relevant environmental conditions. The fibers were tested in a full-size activated carbon respiratory cartridge simulator. The cartridge simulator contained two sampling ports for a conventional gas chromatograph (GC), one at the middle of the bed of activated carbon (mid bed) and a second located at the air outlet of the box (end bed). Three holes were included in the cartridge chamber to accommodate the fiber sensors, and the entire assembly was placed in a stainless steel containment vessel.

Three porous Si capped fibers containing the Si-H, Si-O-Si, and Si-C surface chemistries described above were positioned at the mid-point of the carbon bed and air containing 500 ppm isopropanol was passed through the chamber. The responses of the porous Si sensors and the GC probes are presented in **Figure 7**. The position of the reflectivity peak of the sensors was monitored in the carbon bed with no air flow for 5 min to achieve a baseline. The reflectivity peak position of the sensors remained constant during this period. Air flow (containing isopropanol at a relative humidity of ~36%) was then initiated at a rate of 32 L min^{-1} for 5 min (time = 0 in Figure 7). The reflectivity peak of the Si-O-Si porous Si sample displays an initial blue shift as the humidity in the carbon bed stabilizes (RH for ambient laboratory air = 42%, conditioned air = 36%, measured by a EdgeTech Dewmaster chilled mirror hygrometer, West Wareham, MA). As demonstrated above (Figure 6), the Si-C and Si-H sensors show a much lower dependence on relative humidity, and the signal from these two sensors is relatively stable during the transition from RH = 42% to RH = 36%. After ~75 min of isopropanol vapor flow, the porous Si-tipped fiber sensors display a gradual red shift of the reflectivity peak, indicating the breakthrough of isopropanol into the region of the carbon bed occupied by the fiber sensors. The magnitude of the red shift is consistent with a 500 ppm isopropanol concentration, based on the calibrations discussed in Sec. 2.5 and shown in Figure 5. Detection of isopropanol by the fiber sensors is confirmed by the response recorded from the two GC probes placed mid-bed and at the outlet end of the carbon bed. The ~30 min delay of the mid-bed GC measurement relative to the signals from the three fiber sensors is attributed to slight positional differences of the fibers and the GC probe within the carbon bed.

The improvement in stability afforded by the two chemistries (Si-O-Si and Si-C) is apparent in the response traces of Figure 7. The as-etched porous Si particle (Si-H) displays a significant blue shift during the course of the dosing run. This is attributed to oxidation of the hydride material. Conversion of the Si

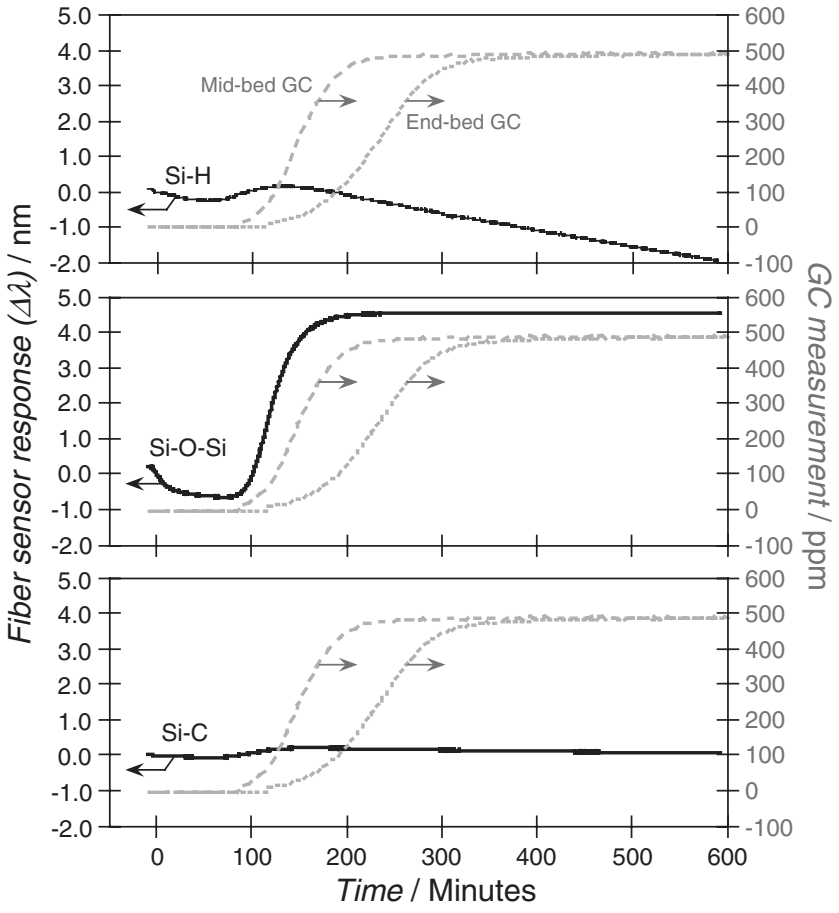

Figure 7. Response of porous Si optical sensors embedded in a carbon bed, demonstrating the detection of isopropanol breakthrough. Vapor breakthrough is monitored by gas chromatograph (GC) probes (right y-axis) at mid bed (gray long dash) and at the outlet of the bed (gray short dash), and by fiber-mounted porous Si sensors (left y-axis) that consisted of chemistries: (top) as-etched (Si-H), (middle) thermally oxidized (Si-O-Si), and (bottom) thermally reacted with acetylene at 485 °C (Si-C). Optical sensor data points were obtained every 20 sec. GC data points were obtained every 4 min. 500 ppm isopropanol flow was initiated at time = 0 in a carrier gas of air at 36% relative humidity.

component of the porous Si matrix to silicon oxide results in a decrease in refractive index of the material, which is manifested as a blue shift in the spectral resonance. The samples with Si-O-Si or Si-C chemistries do not display such a blue shift, consistent with the known stability of these two surfaces.[23,52]

3. Conclusions

Surface chemistry has a pronounced effect on analyte response in porous Si-based optical sensors. When challenged with two VOC analytes intended to probe surface hydrophobicity/hydrophilicity, all but one of the sensor types tested responded more strongly to the hydrophilic analyte (isopropanol) than to the hydrophobic analyte (heptane). A "hydrocarbonized" surface prepared by thermal decomposition of acetylene on an as-prepared porous Si sample responds more strongly to the hydrophobic analyte. When stored in ambient conditions (laboratory air), all of the surface chemistries tested in this work display a stable response to the VOCs heptane and isopropanol over a period of 15 days, although response of the thermally oxidized (Si-O-Si) sample only stabilizes after 8 days of storage in air. Although they provide stable sensor responses, analysis by FTIR indicates substantial changes in the surface chemistry of dodecyl terminated ($Si\text{-}(CH_2)_{11}CH_3$) and methyl terminated ($Si\text{-}CH_3$) samples, which suggest that these sample types may not be appropriate for longer-term environmental monitoring applications. Native porous Si (Si-H) reacts with air and displays significant drift during atmospheric testing. Dimethylsiloxy-terminated ($Si\text{-}O\text{-}Si(CH_3)_2\text{-}O\text{-}Si$), acetylated at 485 °C (Si-C), and thermally oxidized (Si-O-Si) samples appear most suitable for environmental monitoring. A small (sub-mm) particle of either the Si-C or the Si-O-Si surface chemistry can be attached to the distal end of an optical fiber with minor degradation in optical sensor response. The two different sensor chemistries display divergent responses to the isopropanol and heptane analytes used in this study: the Si-O-Si chemistry shows a greater response to isopropanol than to heptane vapors, whereas the Si-C chemistry responds more strongly to heptane than to isopropanol vapors. The results suggest that such chemistries can be used to classify different analytes in a microsensor system. The Si-C modified (acetylated at 485 °C) porous Si sensor displays the lowest response to humidity of the fiber sensors tested. Although significantly reduced, the response of this material to changing RH must still be considered in the design of sensors that are intended to operate in open environments. The feasibility of the fiber-mounted sensors for monitoring service life in an activated carbon respirator cartridge was demonstrated in this and previous work.[23,52] By automating the determination of end-of-service life, the burden is shifted away from the user. The current procedure dictates the use of models or laboratory data to determine service time. It can be complicated for the user since it requires chemical identity, concentration, temperature, work rate and carbon data to make those calculations. Thus automation has the potential to enhance safety and health of respirator users.

4. Experimental Section

Materials: Single-crystalline highly doped p-type Si wafers (0.0008–0.0012 Ω–cm resistivity, (100) polished, B-doped) were purchased from Siltronix Corp. All reagents were used as-received unless otherwise noted. Aqueous HF (49%), isopropanol, acetic acid, undecylenic acid and lithium iodide were purchased from VWR International, West Chester, PA. Heptane, dodecene, iodomethane and silanization solution I (~5% dichlorodimethylsilane in heptane) were purchased from

Sigma-Aldrich, Inc, St. Louis, MO. Absolute ethanol was purchased from Rossville Gold Shield Chemical Company, Hayward, CA. Acetonitrile was purchased from EM Sciences, Hyannis Point North Vancouver, British Columbia V7H 1R9 Canada, purified using a two-column solid-state purification system (Glasscontour System, Irvine, CA), transferred to a glovebox (Vacuum Atmospheres Company, Hawthorne, CA) without exposure to air, and stored over activated molecular sieves. Oxygen was purchased from Westair Gases & Equipment, acetylene from Airgas, Inc., and nitrogen from Praxair, Inc, all from San Diego, CA. Optical fibers (600 micron silica core, low OH) were purchased from Thorlabs, Inc., Newton, NJ. Liquid epoxy resin (Epotuf 37–140, diglycidyl ether of bisphenol-A) was provided by Reichhold, Inc., Research Triangle Park, NC, Curing agent (Ancamine 2432) was provided by Air Products and Chemicals, Inc., Lancaster, PA.

Sensor Construction: Porous Si samples containing a single spectral reflectance peak were prepared by anodization of highly doped p-type Si wafers in a 3:1 v:v solution of aqueous hydrofluoric acid:ethanol in a two-electrode configuration using a platinum ring counter-electrode. Etching was performed in a Teflon etching cell using a galvanostat (Princeton Applied Research Model 363, Oakridge, TN) under computer control (LabView, National Instruments, Austin, TX). The porous layer was etched using a sinusoidal current density waveform varying between 13.3 and 66.4 mA cm^{-2} with a period ranging between 8 and 11.5 s for an etch duration ~10 min. The electrolyte solution was mixed during the etching process to minimize hydrogen bubble formation on the sample surface and to encourage etchant solution exchange in the porous film.[14] Fiber sensors required the detachment of the porous layer from the bulk Si. The porous layer was detached by applying a current of 3.8 mA cm^{-2} for 8 min. in a 3.3% hydrofluoric acid in ethanol solution. Free-standing porous Si was attached to optical fiber with partially cured mixture of bisphenol A epoxy and modified aliphatic amine curing agent and allowed to cure for two days before use.

Gravimetric Determination of Porosity: Five repetitions of each sample etch type were prepared. Samples were weighed before etching (m_1), after etching (m_2), and after dissolving the porous layer with a 0.1M basic solution of KOH in water and ethanol (m_3). The following equation was used to determine the porosity fraction:[29]

$$Porosity\ Fraction = \frac{m_1 - m_2}{m_1 - m_3} \quad (2)$$

Scanning Electron Microscopy: Porous layer thickness was measured with a Phillips XL30 environmental scanning electron microscope (SEM) imaging in secondary electron mode. An accelerating voltage of 10 keV was used. Porous Si tipped optical fibers were sputter-coated with chromium prior to acquisition to avoid sample charging.

Surface Modifications: Thermally oxidized samples (Si-O-Si) were prepared by inserting as-prepared H-terminated porous Si samples (Si-H) in a tube furnace (Lindberg/Blue M, Thermo Fisher Scientific, Waltham, MA) under air at 600 °C for 90 min. Ozone oxidation (Si-OH) was achieved by placing as-prepared Si-H samples in a flowing stream of ozone (Ozone Solutions, product ID OZV-8, flux of 8 g h^{-1}) for 4 min. Silanization of samples (Si-O-Si$(CH_3)_2$-O-Si) was performed by the immersion of ozone oxidized samples in ~5% dichlorodimethylsilane in heptane under inert conditions on a Schlenk line. The samples were heated to 105 °C for 8.5 hours, cooled, and rinsed with dichloromethane and ethanol. Porous samples were functionalized with dodecene (Si-$(CH_2)_{11}CH_3$) via a hydrosilylation reaction.[13] Samples were placed in a flask and covered with neat dodecene. The flask was subjected to three freeze-pump-thaw cycles on a Schlenk line (vacuum gas manifold). Samples were heated to 150 °C under nitrogen for 3 h, then cooled and rinsed with dichloromethane and ethanol. Si-CH_3 samples were prepared from Si-H samples by reductive electrochemical grafting of CH_3I.[17] The Si-H sample was placed in an electrochemical cell with a glass cap fitted with a stopcock and a counter electrode feed-through. The vessel was attached to a Schlenk line and filled with nitrogen. The sample (working electrode) and the Pt counter electrode were then immersed in 4 mL of acetonitrile containing 0.2 M iodomethane and 0.2 M lithium iodide. A cathodic current of 5 mA cm^{-2} was applied for 2 min. Several types of acetylated samples (Si-C) were prepared, by performing the acetylation reaction at various temperatures: an Si-H sample was placed in a ceramic boat and inserted into a tube furnace under a nitrogen flow of 2 L min^{-1}. After 10 min, the furnace was set to the desired temperature (300, 485 or 500 °C). Once the furnace reached the temperature set point, acetylene gas was introduced to the samples at a flow rate of 1 L min^{-1}. After 30 min, the acetylene flow was terminated and the oven was allowed to cool to room temperature.

Infrared Spectroscopy: Surface modification was verified through attenuated total reflectance Fourier-transform infrared (ATR-FTIR) spectroscopy. Spectra were recorded using a Thermo Scientific Nicolet 6700 FTIR with a Smart iTR diamond ATR attachment. Spectral resolution was 4 cm^{-1} and 64 interferograms were averaged per spectrum.

Water Contact Angle Measurements: Sessile drop contact angle measurements were collected on three samples of each surface chemistry, using a digital camera and Adobe Photoshop CS2 for analysis. Using a glass syringe, a 5 µL drop of deionized (Millipore) water was delivered to the chip surface to form a water droplet. Contact angles were measured on both sides of the droplet and averaged.

Vapor Dosing Measurements: Reflectance spectra were collected with an Ocean Optics USB2000 spectrometer, Dunedin, FL, coupled to a bifurcated fiber optic cable. Porous Si chips were probed with a microscope objective lens coupled to the bifurcated cable. Spectra of the fiber-mounted porous Si samples were obtained by coupling the optical fiber to the bifurcated fiber optic cable with a standard fiber coupler. Samples were illuminated with a tungsten halogen (Ocean Optics LS-1) light source. Porous Si chips were exposed to 500 ppm IPA and heptane using a computer-controlled gas dosing system. Nitrogen carrier gas was set to a flow rate of 1.5 L min^{-1} using a mass flow controller (Alicat Scientific, Tucson, AZ). Analyte was injected with a low-volume liquid flow pump (Valco M6, Houston, TX) into a brass block heated to ~45 °C. Porous silicon tipped optical fibers were exposed to analyte vapors under a flow of air. Air flow rate was set at 32 L min^{-1} using a Miller Nelson HCS-401 air conditioning system (Miller Nelson Instruments, a unit of assay technology, Livermore, CA). Analyte was injected as described above. Breakthroughs of activated carbon beds were performed with a custom built APR cartridge simulator consisting of a stainless steel box with inlet and outlet threaded ports on the top and bottom faces for introducing air flow. Inside the box was a small cylinder with a removable top and bottom containing 50 g of activated carbon. Diagrams and description are provided in the Supporting Information.

Supporting Information

Supporting Information is available online from Wiley InterScience or from the author.

Acknowledgements

This work was supported by the National Institute for Occupational Safety and Health and by the National Science Foundation under Grant No. DMR-0806859. Mention of any company, product, policy, or the inclusion of any reference does not constitute endorsement by the National Institute for Occupational Safety and Health. The findings and conclusions of this manuscript are those of the authors and do not necessarily represent the views of the National Institute for Occupational Safety and Health. A.M.R. thanks the University of California, San Diego for a Graduate Assistance in Areas of National Need (GAANN) fellowship. B.H.K and A.M.R. thank the University of California, San Diego for California Space Grant Consortium graduate fellowships. The authors thank Ryan Anderson for help with the SEM images.

Received: March 25, 2010
Revised: May 24, 2010
Published online:

[1] J. M. Lauerhaas, G. M. Credo, J. L. Heinrich, M. J. Sailor, *J. Am. Chem. Soc.* **1992**, *114*, 1911.
[2] J. M. Lauerhaas, M. J. Sailor, *Science* **1993**, *261*, 1567.
[3] C. A. Canaria, M. Huang, Y. Cho, J. L. Heinrich, L. I. Lee, M. J. Shane, R. C. Smith, M. J. Sailor, G. M. Miskelly, *Adv. Funct. Mater.* **2002**, *12*, 495.
[4] R. B. Bjorklund, S. Zangooie, H. Arwin, *Appl. Phys. Lett.* **1996**, *69*, 3001.
[5] P. A. Snow, E. K. Squire, P. S. J. Russell, L. T. Canham, *J. Appl. Phys.* **1999**, *86*, 1781.
[6] R. C. Anderson, R. S. Muller, C. W. Tobias, *Sens. Actuators* **1990**, *A21-A23*, 835.
[7] E. J. Connolly, B. Timmer, H. T. M. Pham, J. Groeneweg, P. M. Sarro, W. Olthuis, P. J. French, *Sens. Actuators B* **2005**, *109*, 44.
[8] S. Zangooie, R. Jansson, H. Arwin, *J. Appl. Phys.* **1999**, *86*, 850.
[9] S. Content, W. C. Trogler, M. J. Sailor, *Chem. Europ. J.* **2000**, *6*, 2205.
[10] J. H. Song, M. J. Sailor, *J. Am. Chem. Soc.* **1997**, *119*, 7381.
[11] M. J. Sailor, in *Properties of Porous Silicon*, Vol. *18* (Ed: L. Canham), Institution of Engineering and Technology, London **1997**, 364.
[12] L. Canham, *Properties of Porous Silicon*, Vol. *18*, Institution of Engineering and Technology, London **1997**.
[13] J. M. Buriak, *Chem. Rev.* **2002**, *102*, 1272.
[14] M. G. Berger, R. Arens-Fischer, M. Thoenissen, M. Krueger, S. Billat, H. Lueth, S. Hilbrich, W. Theiss, P. Grosse, *Thin Sol. Films* **1997**, *297*, 237.
[15] J. M. Buriak, *Chem. Commun.* **1999**, *12*, 1051.
[16] J. H. Song, M. J. Sailor, *Comments Inorganic Chem.* **1999**, *21*, 69.
[17] C. Gurtner, A. W. Wun, M. J. Sailor, *Angew. Chem.Int. Ed.* **1999**, *38*, 1966.
[18] M. R. Linford, P. Fenter, P. M. Eisenberger, C. E. D. Chidsey, *J. Am. Chem. Soc.* **1995**, *117*, 3145.
[19] J. M. Buriak, M. J. Allen, *J. Am. Chem. Soc.* **1998**, *120*, 1339.
[20] M. P. Stewart, J. M. Buriak, *Angew. Chem.Int. Ed. Engl.* **1998**, *37*, 3257.
[21] A. M. Ruminski, M. M. Moore, M. J. Sailor, *Adv. Funct. Mater.* **2008**, *18*, 3418.
[22] J. Salonen, E. Laine, L. Niinisto, *J. Appl. Phys.* **2002**, *91*, 456.
[23] J. Salonen, M. Bjorkqvist, E. Laine, L. Niinisto, *Appl. Surf. Sci.* **2004**, *225*, 389.
[24] J. Salonen, J. Tuura, M. Bjorkqvist, V. P. Lehto, *Sens. Actuator B-Chem.* **2006**, *114*, 423.
[25] M. Bjorkqvist, J. Paski, J. Salonen, V. P. Lehto, *IEEE Sens. J.* **2006**, *6*, 542.
[26] M. Bjorkqvist, J. Paski, J. Salonen, V. P. Lehto, *Phys. Status Solidi A-Appl. Mat.* **2005**, *202*, 1653.
[27] M. Bjorkqvist, J. Salonen, E. Laine, *Appl. Surf. Sci.* **2004**, *222*, 269.
[28] M. J. Sailor, J. R. Link, *Chem. Commun.* **2005**, 1375.
[29] A. Halimaoui, in *Properties of Porous Silicon*, Vol. *18* (Ed: L. Canham), Institution of Engineering and Technology, London **1997**, 12.
[30] N. Masayuki, *J. Am. Ceram. Soc.* **1984**, *67*, C.
[31] C. J. Brinker, E. P. Roth, G. W. Scherer, D. R. Tallant, *J Non-Cryst Solids* **1985**, *71*, 171.
[32] C. J. Brinker, S. P. Mukherjee, *JF – Journal of Materials Science* **1981**, *16*, 1980.
[33] J. Salonen, V. P. Lehto, M. Bjorkqvist, E. Laine, L. Niinisto, *Phys. Status Solidi A-Appl. Res.* **2000**, *182*, 123.
[34] J. E. Bateman, R. D. Eagling, D. R. Worrall, B. R. Horrocks, A. Houlton, *Angew. Chem.Int. Ed.* **1998**, *37*, 2683.
[35] J. Paski, M. Bjorkqvist, J. Salonen, V.-P. Lehto, *Physica status solidi (c)* **2005**, *9*, 3379.
[36] T. Jalkanen, V. Torres-Costa, J. Salonen, M. Björkqvist, E. Mäkilä, J. M. Martínez-Duart, V.-P. Lehto, *Opt. Express* **2009**, *17*, 5446.
[37] B. H. King, A. M. Ruminski, J. L. Snyder, M. J. Sailor, *Adv. Mater.* **2007**, *19*, 4530
[38] T. A. Schmedake, F. Cunin, J. R. Link, M. J. Sailor, *Adv. Mater.* **2002**, *14*, 1270.
[39] J. R. Link, M. J. Sailor, *Proc. Nat. Acad. Sci.* **2003**, *100*, 10607.
[40] *NIOSH Pocket Guide to Chemical Hazards*, National Institute of Occupational Safety and Health of the United States, Publication #2005–149, **2005**.
[41] B. Lee, *Optical Fiber Technology* **2003**, *9*, 57.
[42] S. M. Barnard, D. R. Walt, *Environ. Sci. Technol.* **1991**, *25*, 1301.
[43] J. A. Ferguson, B. G. Healey, K. S. Bronk, S. M. Barnard, D. R. Walt, *Analytica Chimica Acta* **1997**, *340*, 123.
[44] J. R. Epstein, D. R. Walt, *Chemical Society Reviews* **2003**, *32*, 203.
[45] O. S. Wolfbeis, *Anal. Chem.* **2006**, *78*, 3859.
[46] J. A. Ferguson, T. C. Boles, C. P. Adams, D. R. Walt, *Nat. Biotechnol.* **1996**, *14*, 1681.
[47] D. R. Walt, *Science* **2000**, *287*, 451.
[48] K. L. Brogan, D. R. Walt, *Current Opinion in Chemical Biology* **2005**, *9*, 494.
[49] S. Caron, P. Bernard, M. Vernon, J. Lara, *Sensors and Actuators B: Chemical* **2004**, *102*, 198.
[50] NIOSH, *Certification Criteria* **2005**, *Procedure No. RCT-APR-STP-0066.*
[51] OSHA, Vol. Standard 1910.134(d)(3)(iii)(B)(2), U.S. Department of Labor, **2006**.
[52] M. P. Schwartz, S. D. Alvarez, M. J. Sailor, *Anal. Chem.* **2007**, *79*, 327.
[53] A. Kurokawa, S. Ichimura, *Appl. Surf. Sci.* **1996**, *100/101* 436.
[54] T. Gao, J. Gao, M. J. Sailor, *Langmuir* **2002**, *18*, 9953.